

Acceleration of UHE cosmic rays in gamma-ray bursts

G. Pelletier^{1,2} and E. Kersalé¹

¹ Laboratoire d’Astrophysique de l’Observatoire de Grenoble, B.P. 53, 38041 Grenoble cedex 9, France

² Institut Universitaire de France

Received 3 April 2000 / Accepted 30 May 2000

Abstract. Gamma-Ray Bursts are good candidates of the “bottom up” scenario for the generation of the UHE Cosmic Rays. In the most discussed model of GRBs, namely the “fireball” model, a highly relativistic shock forms and seems capable of accelerating the cosmic rays up to the EeV range. However, only the first Fermi cycle produces a large energy gain to particles coming from the external medium. Thus, a complementary acceleration is proposed, downstream of the external shock, in the relativistic plasma of the GRBs, where crossings of relativistic fronts are likely to occur. Both forward and backward fronts are necessary for the internal Fermi acceleration to work and the physical process that generates them is presented. We found that there exists a relevant physical process similar to Brillouin backscattering that redistributes the incoming energy in the plasma shell. This redistribution occurs through the generation of sound waves that heat the plasma shell and also through the generation of both forward and backward relativistic Alfvén fronts that accelerate cosmic rays by the Fermi process. We show that this ensemble of processes is able to account for the generation of UHE cosmic rays.

There are two opportunities for these combined processes, first during the “primary” Gamma-Ray Burst where baryons are entrained by the relativistic pair wind, second during the predeceleration and deceleration stages when the fireball interacts with the interstellar medium. However, because of the synchrotron losses, only the second stage can produce the UHE cosmic rays.

Key words: gamma rays: bursts – ISM: cosmic rays – acceleration of particles – instabilities

1. Introduction

The origin of the cosmic ray population beyond $10^{15} eV$ is an important enigma of modern astrophysics which will hopefully be clarified by the Pierre Auger instrument. Beyond this energy, the galactic magnetic field is unable to scatter cosmic rays and moreover supernovae remnants cannot accelerate protons. Pulsars could accelerate protons up to $10^{17} eV$. This population,

that has an isotropic energy spectrum with a powerlaw index 3.1, probably comes from extragalactic sources. The “knee” of the spectrum around $10^{15} eV$ is so smooth that the extragalactic contribution could be important at lower energy also.

The photoproduction of pions by cosmic ray protons on the Cosmic Microwave Background, the GZK-effect, occurs beyond the energy threshold of $3 \times 10^{19} eV$ and higher energy protons cannot come from sources located farther than $100 Mpc$ (Aharonian & Cronin 1994). Few events beyond the GZK-threshold have recently been detected by AGASA (Hayashida et al. 1998) and the “Fly’s eyes” (Sokolosky 1998), and the Auger experiment will considerably improve the statistics of these events. These preliminary results suggest that a new population of cosmic rays is observed at energies higher than $10^{18} eV$, because the spectrum becomes harder. The origin of these few events, although some pointing ability of the instruments, remains very uncertain. The identified extragalactic sources within $100 Mpc$ are very few.

Vietri (1995) and Waxman (1995) showed that the rate of GRBs in the Universe ($10^{-8} yr^{-1} Mpc^{-3}$) and their energy ($10^{51} - 10^{53} erg$) make them very good candidates as sources of the UHECRs, if 10% of their energy is converted into UHECR energy. The most considered GRB model, namely the “fireball” model (Rees & Mészáros 1992), is based on a relativistic blast wave having a Lorentz factor Γ_s larger than 10^2 , this high value being necessary for gamma photons to escape from pair production. A Fermi cycle at a relativistic shock can amplify the energy of cosmic ray by a factor Γ_s^2 . Thus two Fermi cycles could be sufficient to reach the expected energy of the UHECRs. However, Gallant & Achterberg (1999) recently showed that only the first cycle can produce such amplification, the next cycles amplifying by a factor of 2 only. Moreover the escape probability is large (0.3–0.5).

The GRB light curves indicate strong internal disturbances and they have been considered as the main cause of gamma-ray emission and a possible cause of cosmic ray generation (Waxman & Bahcall 1999; Daigne & Mochkovitch 1998). In this paper we propose an interpretation of these disturbances in terms of relativistic hydromagnetic fronts, calculate their generation through the streaming instability caused by baryon loading, show that there is an efficient nonlinear generation of both forward and backward waves, estimate the amount of energy

they extract from the fireball and calculate the acceleration of cosmic rays by their crossings. The baryon loading occurs first during the “primary” GRB when the relativistic pair wind entrains the debris of the progenitor, and then during the interaction of the fireball with the interstellar medium. Furthermore, the first loading is likely to occur in the “hypernova” scenario, however, this is less obvious in the “merging” scenario.

2. Loading baryons

The canonical fireball model (Rees & Mészáros 1992) presents a primary explosion during which the plasma is optically thick until t_* ($R_* = ct_*$), then an adiabatic and free expansion until the ambient medium starts to exert sufficient ram pressure; this defines a deceleration time t_d and a deceleration radius R_d (typically $t_* = 3 \times 10^{-3} t_d$). The third stage is thus the deceleration one during which most of the energy of the fireball is dissipated in the interstellar medium, giving rise to the afterglow. We assume that the fireball is initially composed of $e^+ - e^-$ pairs and that this ultra-relativistic wind of bulk Lorentz factor Γ , flowing along a strong poloidal magnetic field, is perturbed by ambient baryons of mass density ρ_b . There are two stages of baryon loading, during the “primary” GRB and during the interaction with the interstellar medium.

2.1. Hydrodynamics of the baryon loading stage

The main features of the hydrodynamics of the relativistic fireball can be derived from the energy invariant as long as the radiation losses are negligible (assuming radial magnetic field lines):

$$E = \int (e + \beta^2 P) \gamma^2 d^3v, \quad (1)$$

where e is the comoving energy-mass density, P the comoving pressure, β the flow motion (in unit of light velocity), and γ the Lorentz factor of the flow ($\gamma \equiv (1 - \beta^2)^{-1/2}$), distributed around the typical bulk Lorentz factor Γ . We assume that the plasma shell is composed of a low pressure baryonic component of mass M and a high pressure relativistic component containing pairs and cosmic rays of average energy density in comoving frame $e_* = 3P$. We approximate the energy by the following expression, assuming an appropriate self-similar evolution of the shell (which allows us to properly define the bulk Lorentz factor):

$$E = M\Gamma c^2 + 4P\Gamma V_0, \quad (2)$$

where $V_0 = 4\pi R^2 \delta R_0$ is the covolume of the shell, $R(t)$ the shell radius, δR_0 its comoving thickness. During the expansion, the energy in the shell is redistributed between kinetic and internal energies through the competition of adiabatic cooling and heating by the flux of incoming matter. Part of the mass flux increases the low pressure baryonic mass: $\dot{M} = (1 - \alpha)\rho_b \Gamma c 4\pi R^2$; the other part contributes to the high energy component: $\dot{e}_*|_{heating} = \alpha\rho_b \Gamma c^3 4\pi R^2 / V_0$, assuming a

heating length shorter than the fireball width. The adiabatic cooling is such that $\dot{e}_*|_{adiab} = -\frac{4}{3}\frac{\dot{V}_0}{V_0}e_*$. Thus setting $\dot{E} = 0$, after some simple manipulations, we obtain (with $\alpha_0 \equiv 1 + \alpha/3$):

$$\alpha_0 \rho_b 4\pi R^2 c^3 \Gamma^2 + \frac{1}{3} \frac{\dot{V}_0}{V_0} M \Gamma c^2 + \left(\frac{\dot{\Gamma}}{\Gamma} - \frac{1}{3} \frac{\dot{V}_0}{V_0} \right) E = 0. \quad (3)$$

It can easily be checked that, when there is no mass input, an adiabatic expansion occurs such that $\Gamma = \Gamma_0 (V_0(t)/V_0(t_0))^{1/3}$ as long as $M\Gamma c^2 \ll E$, followed by a free expansion $\Gamma \simeq E/Mc^2$ when the internal energy has become smaller than the kinetic energy. Now to analyze the effect of the mass sweeping, we assume a self-similar expansion such that $d \ln V_0 / d \ln t = \chi$ and define the dimensionless quantity $\eta(t)$ (within a coefficient of order unity) as the ratio of the fireball energy over the swept energy-mass of the ambient medium, measured in the comoving frame, such that

$$E = \eta(t) \rho_b \frac{4}{3} \pi R^3 \Gamma^2 c^2. \quad (4)$$

Then Eq. (3) leads to the differential equation:

$$\frac{d\eta}{d \ln t} = 2\eta(\eta_\infty - \eta), \quad (5)$$

where η_∞ is the asymptotic value taken by $\eta(t)$, namely $\eta_\infty = \frac{3}{2} + \frac{\chi}{3}$. With $\eta(t_0) = \eta_0$, the solution is

$$\eta(t) = \eta_\infty \frac{\eta_0 (t/t_0)^{2\eta_\infty}}{\eta_\infty - \eta_0 + \eta_0 (t/t_0)^{2\eta_\infty}}. \quad (6)$$

The evolution starts in the adiabatic regime, $\eta(t) \simeq \eta_0 (t/t_0)^{2\eta_\infty}$ and $\Gamma \propto t^{\chi/3}$. If η reaches its asymptotic value, then the bulk Lorentz factor decreases according to the canonic law $\Gamma \propto t^{-3/2}$. However, the interest of this derivation is to stress that this Blandford & Mc Kee (1976) law does not mean that a free expansion has been reached and a strong relativistic shock set up. Indeed the energy of the fireball can still be dominated by the internal energy, so that a shock does not form, and the incoming baryons interact with the fireball plasma through a streaming instability. This is probably what happens during the primary stage of baryon loading where a high entropy pair plasma entrains some baryonic mass, expected to be of the order $10^{-6} M_\odot$, coming from the debris of the progenitor. This interaction is probably more important than the final stage of interaction with the interstellar medium in generating perturbations in the flow as described in Sect. 2.3 and Sect. 3.

Thus there are two stages of baryon loading (see Fig. 1), the primary stage when the high entropy pair wind entrains a mass $M_0 \sim 10^{-6} M_\odot$ coming from the debris of the massive star giving rise to the hypernova or of the merging compact objects, and a secondary stage corresponding to the sweeping of the ambient interstellar medium but that loads typically $10^{-3} M_0$ only.

2.2. The magnetic field and some scales

We assume that this baryonic plasma flows along a strong poloidal magnetic field. This is the major assumption of this

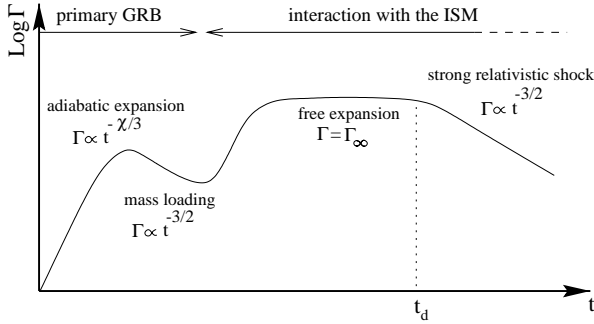


Fig. 1. Evolution in time of the Lorentz factor Γ . The deceleration giving rise to the afterglow starts at time t_d , after a free expansion involving the asymptotic bulk Lorentz factor $\Gamma_\infty = E/Mc^2$.

paper: $B > B_{eq}$ (we note $\beta_p \equiv (B_{eq}/B)^2 < 1$) and $B > B_m$ where B_{eq} is the equipartition field corresponding to the plasma pressure in the fireball, and B_m is the equipartition field corresponding to the ram pressure exerted by the incoming baryons.

$$B_m \simeq 10^2 \left(\frac{n_b}{1 \text{ cm}^{-3}} \right)^{1/2} \frac{\Gamma}{10^3} \text{ Gauss}. \quad (7)$$

Indeed, the poloidal magnetic pressure follows the same decrease as the relativistic pressure with distance; for conical expansion, $B_p^2/8\pi \propto P \propto R^{-4}$. Moreover, a toroidal magnetic field is likely significant in the edge of the collimated flow and can play a confining role. The decay of the toroidal field is weaker, because $B_t \propto R^{-1}$ in a conical expansion. If the magnetic field dominates at the beginning, it remains so with the expansion. Moreover, a tiny initial toroidal component of the magnetic field can become dominant in the expansion and favors collimation. Like in extragalactic jets, the poloidal field can be dominant along the axis of the flow and the toroidal field dominant in the edge of the flow. Thus we assume an internal poloidal field such that $B_p = B_d(R/R_d)^{-2}$ with $B_d \gtrsim B_m$ at $R_d \sim 10^{16} \text{ cm}$ and an external toroidal field $B_t \gtrsim B_d(R/R_d)^{-1}$; in particular at R_* (typically $10^{-3}R_d$), $B \sim 10^8 \text{ G}$. Of course these estimates are sensitive to the model of magnetic field distribution, however the numbers we proposed are reasonable and help to explain out what happens.

In the early stage the proton energy is severely limited by synchrotron losses. Assuming an acceleration time $t_{acc} = \kappa t_L$, where t_L is the Larmor time, the maximum proton energy is such that the acceleration time is equal to the synchrotron time and gives

$$\epsilon_{max} = 2 \frac{10^{11}}{\sqrt{\kappa}} \left(\frac{B}{1 \text{ G}} \right)^{-1/2} \text{ GeV}. \quad (8)$$

Taking $\kappa \simeq 10$, the energy of 10^{17} eV can be achieved only in the region where B is smaller than $B_s \simeq 10^6 \text{ G}$, which requires $R > R_s \simeq 10^{-2}R_d$. Bearing in mind that Γ reaches a value between 10^2 – 10^3 , the UHECRs ($\sim 10^{20} \text{ eV}$ in the observer frame) are necessarily produced in the region $R > R_s$.

A neutrino radiation is produced during the early stage through pp-collisions thanks to Fermi acceleration. Indeed, ϵ_{max} given by (8) exceeds 1 GeV when $B < 10^{12} \text{ G}$, therefore

where $R > R_h \sim 10^{-2}R_*$. This low energy neutrino emission ends when the pp mean free path becomes larger than δR , thus when $R = R_{pp} \sim 10^2 R_h \sim R_*$. This stage of Fermi acceleration supports the predictions made by Paczynski & Xu (1994), namely a neutrino emission between $30 \text{ GeV} - \text{TeV}$ of global energy of a few percent of the fireball energy.

2.3. Relaxation of the baryon stream in the fireball

In this subsection, we examine how the backstream of baryons in the fireball, initially composed of $e^+ - e^-$ pairs, undergoes a relaxation by triggering a beam instability in the pair plasma.

The hydromagnetic perturbations so produced scatter the baryons that are then entrained and some of them accelerate to high energy. We presume that these perturbations are those revealed by the light curve and which also accelerate the electrons responsible for the synchrotron and inverse Compton gamma-emission. Indeed, initial perturbations do not amplify in the expansion, they even decay (this differs from an expanding universe that is self-gravitating). Therefore we stress that these perturbations must be generated during the expansion by the appropriate instability.

At the presumed energy of the particles, the Coulomb interactions are negligible (indeed, for relativistic electrons, the Coulomb cross section is as low as the Thomson cross section; as long as the shell is optically thin to Compton scattering, the mean free path is larger than the shell width; this is of course more obvious when protons are involved in the collision). Therefore the incoming baryons interact only with the magnetic field carried by the fireball. The magnetic field represents a more efficient obstacle if it is perpendicular to the flow, and the interaction starts in the form of an intense backward fast magneto-sonic wave. In a confined relativistic plasma, the fast mode propagates with a Lorentz factor $\gamma_F = \gamma_S \gamma_*$, where the sound Lorentz factor (corresponding to the parallel slow mode actually) $\gamma_S = \sqrt{3}/2$ and the Lorentz factor of the generalized Alfvén waves (see Pelletier & Marcowith 1998) $\gamma_* = \left(1 + \frac{1}{2\beta_p}\right)^{1/2}$. However, since we consider a collimated expansion, the most natural circumstance is the interaction along the parallel magnetic field within a wide solid angle around the axis.

In this scope, the interaction scenario is the following. In the comoving frame, the proton back-stream, of velocity $v_b = \beta_b c$ and Lorentz factor Γ_b , along the field line generates backward Alfvén waves of velocity $V_* = \beta_* c$ at a rate g given by (Marcowith et al. 1997; Pelletier & Marcowith 1998):

$$g = g_0 \frac{\Gamma}{\Gamma_b} \sqrt{\beta_b - \beta_*}, \quad (9)$$

where $g_0 \equiv \frac{\omega_{pi}}{\Gamma} (2\beta_*)^{-1/2}$, ω_{pi} being the plasma frequency of the ions in the stream. This maximum growth occurs for the wave number

$$k_0 = \frac{\omega_{ci}}{\Gamma_b(v_b - V_*)} \simeq \frac{\gamma_*^2 \omega_{ci}}{\Gamma_b c}. \quad (10)$$

When these backward waves have reached a high level, they scatter the baryons that are then entrained by the pair flow. Thus,

we presume that the large internal disturbances observed in the light curve result from loading baryons in the fireball either at the early stage of the explosion or during the “free” expansion stage. At the beginning of the fireball expansion in the interstellar medium, the diffusion length is not short enough compared to the narrow width of the shell. Then baryon entrainment starts when the level of the resonant Alfvén waves (hereafter A-waves) is strong enough to get a diffusion length shorter than the shell thickness. Then the kinetic flux of the incoming baryons is transformed into a backward flux of intense A-waves. As long as these waves do not interact with the plasma shell (their wavelengths are larger than the dissipation scale), the shell does not decelerate and just an electromagnetic wake is generated propagating towards to shell center but more slowly than the ultrarelativistic expansion of the shell so that it seems to advance. Thus for a baryon mass loading rate $\dot{M}_b = 4\pi R^2 \rho_b \Gamma c$, the energy flux, measured in the comoving frame, generated in the form of backward disturbances in the shell is:

$$S = V_* W_* = \frac{\dot{M}_b}{4\pi R^2} \Gamma c^2. \quad (11)$$

For a fireball of initial energy E_0 , this baryon loading produces only a weak shell deceleration as long as

$$t < t_d = \frac{3E_0}{\dot{M}_b \Gamma c^2}, \quad (12)$$

where t_d is the deceleration time. In other words, the shell is still weakly perturbed as long as the mass loading rate is smaller than $\dot{M}_d = \rho_b \Gamma 4\pi R_d^2 c$ where $R_d = ct_d$ is the deceleration radius. There are in fact two deceleration radii corresponding to the two stages of baryon loading.

The relaxation of the baryon stream in the fireball is described by the following simplified model coupling the relative level of Alfvén energy density u with the relative motion of the stream $\beta_b - \beta_*$ with respect to the backward A-waves so-generated. The coordinate r denotes the radial distance from this external sheet, increasing r means approaching the shell center and the “initial” condition is $\Gamma_b(0) = \Gamma$.

$$V_* \frac{du}{dr} = 2gu \quad (13)$$

$$c \frac{d\Gamma_b}{dr} = -\nu \beta \Gamma_b \quad (14)$$

where in a quasi-linear approximation the slowing rate $\nu = \nu_0 u$, the more intense the waves the more efficient the scattering. The energy flux conservation implies that

$$\nu_0 = \frac{2g\Gamma}{u_\infty \beta_* \beta \Gamma_b} \quad (15)$$

where u_∞ is the asymptotic value of u , namely $W_*/(B^2/8\pi)$ given by (11) and thus $u_\infty = (B_m/B)^2 < 1$.

The relaxation of the stream can be characterized by a single typical length $l_r = V_*/g_0$. Fig. 2 illustrates the stream relaxation in the shell that occurs in few l_r .

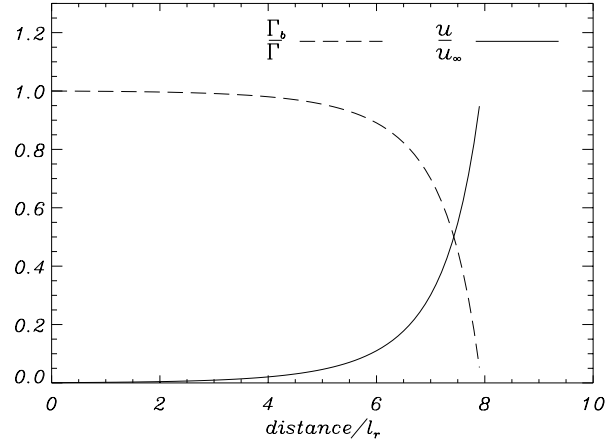


Fig. 2. Stream relaxation and growth of the waves. The final relaxation stage, for $\beta < \beta_*$, is just a fast isotropisation involving plasma microphysics not detailed in this paper. The transition to the non-relativistic regime gives rise to a stiff variation.

Let us consider the interaction with the interstellar medium. The typical wavelength of the excited waves, measured in light seconds ($l.sec.$), is such that

$$\lambda_0 \simeq 10^{-3} \frac{\Gamma}{10^3} \left(\frac{B}{10^3 G} \right)^{-1} l.sec., \quad (16)$$

whereas the relaxation length is

$$l_r \simeq \frac{\Gamma}{10^3} \left(\frac{n_b}{1 cm^{-3}} \right)^{-1/2} l.sec.. \quad (17)$$

This has to be compared with the shell width in the comoving frame; at the deceleration time its estimate is (Rees & Mészáros 1992)

$$\delta R_d \simeq 3 \times 10^2 \left(\frac{n_b}{1 cm^{-3}} \right)^{-1/3} \left(\frac{\Gamma}{10^3} \right)^{-5/3} \times \left(\frac{E}{10^{51} erg} \right)^{1/3} \left(\frac{\Omega}{4\pi} \right)^{-2/3} l.sec..$$

Let us consider now the interaction in the “primary” GRB. Expanding $10^{-6} M_\odot$ within a sphere of one light-second radius (comoving) leads to a particle density of $10^{19} cm^{-3}$. The plasma is now collisional, but the collective process previously developed provides a faster relaxation than both Coulomb and pp-collision ones. The typical wavelength $\lambda_0 \simeq 10^{-10} \frac{\Gamma}{10^3} \left(\frac{B}{10^{10} G} \right)^{-1} l.sec.$ and the relaxation length $l_r \simeq 10^{-9} \frac{\Gamma}{10^3} \left(\frac{n_b}{10^{18} cm^{-3}} \right)^{-1/2} l.sec..$ Incidentally, we note that although the time is quite short, the density is so high that the Lawson criterium for fusion is largely satisfied; moreover the thermal energy of the particles is high ($\bar{\epsilon} \sim 10^{12} eV$). Thus, alpha particles and neutrons should be produced and moreover, as mentioned previously, a significant neutrino emission.

Once the relaxation is achieved, there are two major non-linear interactions with the plasma shell through magnetosonic compression. First, intense backward A-waves that propagate almost parallel to the magnetic field produce fast magnetosonic

compression governed by the Hada's system generalized to relativistic plasma by Pelletier & Marcowith (1998). The transverse magnetic perturbation b (reduced to the averaged field) exerts a pressure that produces fast parallel perturbed motion u_{\parallel} (specific momentum) that is proportional to the parallel electric field (see Pelletier 1999). This, parallel electric field is responsible for particle acceleration or stochastic heating. For delocalized waves, particles that resonate with the parallel electric field produce the nonlinear Landau damping of the A-waves. The so-produced E_{\parallel} efficiently injects electrons and positrons in the high energy population.

There is also another strong nonlinear effect with the slow magnetosonic mode (S-mode) that efficiently backscatters the primary flux of A-waves. This is presented in the next section.

3. Brillouin backscattering

As seen in the previous section, the flux of backward A-waves becomes stronger and stronger as long as the shell is still entraining baryons. If these waves are not be absorbed in the plasma shell, no deceleration nor heating of the shell would stem from the relaxation of the incoming baryons. Moreover, Fermi acceleration with these waves can work only if there are both forward and backward waves. One could expect some reflection of these waves in the internal edge of the shell; however, because they propagate at a velocity close to the light velocity, no significant change of impedance and thus no significant reflection occurs at the edge. Both absorption and backscattering efficiently develop by excitation of sound or slow magnetosonic modes.

3.1. Parametric Brillouin instability

A large fraction of this flux can be backscattered (thus producing a forward A-flux) by exciting the slow mode of the shell plasma. This is analogous to the Brillouin backscattering, but with A-waves instead of ordinary electromagnetic waves. The analogous Raman scattering does not work with A-waves (three mode couplings does not work with A-waves). A mother A-wave (ω_0, k_0) of relative amplitude b_0 spontaneously gives rise to a slow magnetosonic mode (ω_s, k_s), but this S-mode is unable to carry the whole flux of energy-momentum and a backward (forward with respect of the shell expansion) A-wave is generated with a lower energy-momentum (ω_-, k_-) such that:

$$\omega_0 = \omega_s + \omega_- \text{ and } k_0 = k_s + k_- . \quad (18)$$

For parallel propagating resonant waves,

$$k_s = \frac{2k_0}{1 + V_s/V_*} \text{ and } k_- = k_0 \frac{1 - V_s/V_*}{1 + V_s/V_*} , \quad (19)$$

one gets the most efficient rate of coherent wave decay:

$$G_{decay} = \frac{1}{2} \sqrt{\omega_s \omega_-} \left(\frac{b_0^2}{2\beta_p} \right)^{1/2} . \quad (20)$$

This result is a particular solution that can be derived from the complete analysis made by Champeaux et al. (1999). For incoherent scattering, the decay rate is lower, proportional to $b_0^2/2\beta_p$ instead of its square root.

The S-modes are in turn absorbed by resonant interaction with "thermal" particles. This process is clearly the most efficient to transmit the momentum and energy of the baryon stream to the plasma shell.

Now intense forward and backward flux of long A-waves are still remaining. There is no other way to absorb them than cosmic ray acceleration through Fermi processes that involve resonant interaction between high energy particles and long A-waves.

3.2. A toy model of the backscattering process

In principle, solving the nonlinear system that governs the backscattering process allows us to predict how the dissipated energy is shared between heating the thermal particles of the shell and acceleration of cosmic rays. The detailed theory involves the numbers of quanta for each mode (N_+, N_-, N_s) for the mother A-waves, the backscattered A-waves and the generated slow waves respectively), a probability rate of scattering w and absorption rate ($\gamma_+, \gamma_-, \gamma_s$), all these triplets depending of the three wave vectors. In this paper we merely address a very simplified version of the system, similar to the system obtained with random phase approximation, but averaged over the spectral bands. We think it would be useful to solve such a toy system to illustrate the process and to see whether reasonable estimates can be obtained by developing this method. For the sake of simplicity, we assume that backscattering occurs behind the stream relaxation sheet (in fact, it could even start in the relaxation sheet). The system is thus the following (in this notation a backscattered wave propagates outwards):

$$V_* \frac{\partial}{\partial r} N_+ = -w(N_+ N_s + N_+ N_- - N_- N_s) - \gamma_+ N_+ \quad (21)$$

$$-V_* \frac{\partial}{\partial r} N_- = w(N_+ N_s + N_+ N_- - N_- N_s) - \gamma_- N_- \quad (22)$$

$$V_s \frac{\partial}{\partial r} N_s = w(N_+ N_s + N_+ N_- - N_- N_s) - \gamma_s N_s \quad (23)$$

The absorption rate γ_s of the S-waves by the "thermal" plasma is always larger than the absorption rates γ_+ and γ_- of the A-waves by cosmic rays (gyro-synchrotron absorption); moreover the S-waves have shorter wavelengths than the A-waves, the backscattered waves have even larger wavelengths than their mother wave and thus even less absorbed. There are two scales in the system: a short characteristic scale associated to the growth of the S-waves $l_s = V_s/(\gamma_s - G)$, where $G = w(N_+(0) - N_-(0))$ is the nonlinear scattering rate, and a longer scale associated with the decay of the mother waves $l_* = V_*(\gamma_s - G)/\gamma_s G$; $l_s \ll l_*$ when $G \ll \gamma_s$. This decay length $l_* \sim \beta \lambda_0/u$. A ratio T of the incident flux is transmitted, a ratio R is reflected, a ratio A is absorbed and one has:

$$T + R + A = 1 ; \quad (24)$$

and the absorption ratio is divided into a thermal one through S-waves, A_s , and a nonthermal one through A-waves, A_* . Thus when $V_*/\gamma_+ < \delta R$, $T \simeq 0$. By solving the system, one ob-

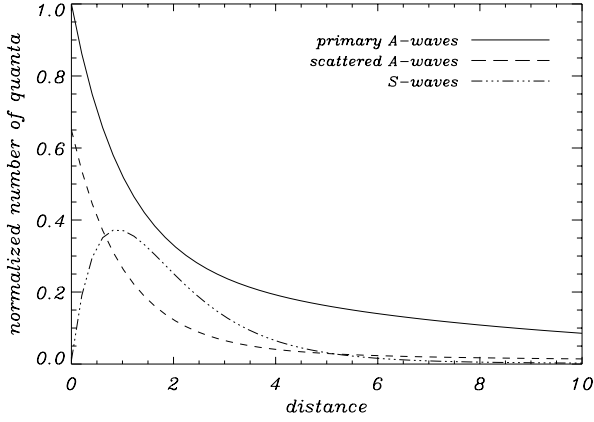


Fig. 3. Solutions of the backscattering system. By order of decreasing line thickness we show $N_+/N_+(0)$, $N_-/N_+(0)$ and $N_s/N_+(0)$. The distance unit is the scattering length defined by $V_*/\omega N_+(0)$. In this example $\gamma_+ = 0.1$, $\gamma_- = 0.05$ and $\gamma_s = 0.69$.

tains the backscattering rate: $R = \frac{\omega_- N_-(0)}{\omega_0 N_+(0)}$. One calculates the thermal absorption ratio:

$$A_s = \frac{\int_0^\infty \gamma_s \omega_s N_s dr}{V_* \omega_0 N_+(0)}. \quad (25)$$

The absorption rate into cosmic rays is deduced by using (24). Such a calculation is illustrated in Fig. 3. For reasonable absorption rates, we obtain $R \simeq 0.17$, $A_s \simeq 0.53$ and $A_* \simeq 0.30$. Of course, a more realistic calculation should be made to predict these ratios, but this simple model indicates that, through the backscattering process, a sizable fraction of incoming energy can be converted into cosmic rays. In particular, a more detailed calculation would take into account that the longer wavelength modes are less damped and thus can be transmitted behind the shell.

The combined process of stream relaxation and Brillouin scattering followed by energy absorption by particles occurs first during the “primary” stage of the relativistic expansion when the pair wind entrains ambient baryons coming from the progenitor debris. As argued previously, this interaction is likely to occur without shock formation. Then after a new adiabatic and free expansion, a new stage of interaction occurs with the interstellar medium. The ratio of the energy dissipated by the cosmic rays acceleration over the initial fireball energy is $E_{cr}/E = A_* R(t)^3 / R_d^3$ before the deceleration time; thus, at $R = 0.3 R_d$, about 10% of the fireball energy is converted into cosmic rays. When the fireball radius reaches the deceleration radius, a strong collisionless shock is set up. However it can be considered as a hardening of the previous process. Indeed, incoming protons are reflected in the relaxation front giving rise of the external shock, whereas the backward magnetosonic wavefronts turn to internal shocks. The previous description applies during the predeceleration stage. However, although the theory of beam-plasma instability is no longer relevant when the shock is set up, the Alfvén fronts are still behind the shock and still accelerate cosmic rays efficiently.

4. Fermi acceleration of UHE cosmic rays

As stressed by Pelletier (1999), intense forward and backward A-waves of long wavelength (delocalized or localized) are necessary to accelerate UHE Cosmic Rays. The intense localized fronts propagate with a nonlinearly modified velocity such that $\gamma_* \mapsto \gamma_{nl} = \gamma_* + \delta\gamma$ with $\delta\gamma/\gamma_* \sim \beta_* b_m^2$ (b_m being the maximum reduced amplitude of the perturbed magnetic field of the front measured in its comoving frame). These intense wave packets scatter particles of Larmor radius smaller than their width or wavelength in their frame in a few gyro-periods. In a scattering time, the particles energy gains a factor γ_*^2 and the momenta are concentrated in the front cone of half-angle $1/\gamma_*$. Further acceleration requires other fronts propagating in the opposite direction, because wavefronts propagating in the same direction at almost the same velocity V_* tend to roughly isotropize the distribution of interacting particles with respect to their comoving frame. Thus it is crucial to get both forward and backward fronts to accelerate cosmic rays and the Brillouin backscattering process of Sect. 3, that generates longwavelength perturbations in a time $\sim G^{-1}$, is the appropriate and efficient solution. The relativistic regime of Fermi acceleration is deeply different from the nonrelativistic regime, not only because of the anisotropy effect but also because the acceleration time scale can become shorter than the scattering time scale. This is a crucial advantage that is illustrated by the following result (Pelletier 1999) obtained in the case of a permanent flux of both forward and backward waves, the energy gain during a time Δt , smaller than the scattering time, is such that

$$\langle \Delta p^2 \rangle = p^2 \beta_*^2 \gamma_*^2 \nu_s \Delta t, \quad (26)$$

where ν_s is the scattering frequency. Moreover, because $B > B_{eq}$, $\gamma_* > 2$, and the energy jump at each scattering is large and the statistic evolution cannot be treated by a Fokker-Planck description.

Let us give some more details about the localized fronts. Intense longwaves tend to self-organize in forward and backward relativistic fronts of amplitude $b_m \sim (r_*/\xi)^{-1/2}$, where ξ is the front width and $r_* = (\langle \gamma^2 \rangle / \bar{\gamma}) V_*/\omega_c$ is the minimum scale of relativistic MHD (Pelletier & Marcowith 1998); it is worth noting that the perturbation amplitudes appear Γ^2 times larger in the observation frame. At each crossing of these fronts, the gain is by a factor γ_*^4 within few gyro-periods. Such localized fronts can be approximately described as solitons (Pelletier & Marcowith 1998; Pelletier 1999), they differ from ideal solitons because of the Fermi acceleration that produces a kind of Landau-synchrotron damping of them. When ideal solitons cross each other they do not destroy, whereas damping destroys them and their complete absorption corresponds to the strongest efficiency of the Fermi process. A similar idea was used by Daigne & Mochkovitch (1998) with internal shocks to explain the gamma emission. Here we interpret the internal shocks as internal Alfvén fronts which can contribute to short scale variations in the light curve, and possibly more easily than pure hydrodynamic shocks.

For a bulk Lorentz factor of the shell of 10^3 , particles in GRBs have to reach $10^{17} eV$ in the comoving frame in order to supply the UHE Cosmic Rays population beyond the GZK threshold. We consider the interaction with the interstellar medium only because, as previously showed, synchrotron losses prevent UHE cosmic ray production, inside a radius R_s (Sect. 2.2). Assuming that the largest wavelengths are one tenth of the effective shell width (limited by causal connection), a magnetic field just larger than the equipartition value at deceleration radius ($B_{eq} \sim 10^3 G$ say) is enough to get Larmor radii of that size (i.e. $\sim 10^{-5} pc$), which corresponds to an energy of order $10^{17} eV$. With $\bar{\gamma} \sim 10^8$, the scale $r_* \sim 10 l.sec.$. Therefore, few fronts having a width of $1-10r_*$ that cross each other within a shell width of $3 \times 10^2 l.sec.$ can produce protons of $10^{21} eV$ within one second with respect of an observer frame during the interaction with the interstellar medium. When the strong relativistic shock has formed ($R > R_d$), external particles gain energy by a first Fermi half-cycle by a factor Γ_s^2 . They are then injected in the relativistic A-fronts behind the shock and suffer further acceleration up to the ultimate energy.

The local distribution is more likely quasi monoenergetic rather than a powerlaw. However the local characteristic energy is proportional to the product BR and thus the global distribution reflects the distribution of the product BR ; as stated by Pelletier (1999), a distribution close to ϵ^{-2} is obtained for $B \propto R^{-m}$ with m close to 2.

Our main conclusion is that Gamma-Ray Bursts are capable of producing the UHE Cosmic Rays through a Fermi process with relativistic Alfvén waves. These intense waves are generated by the two stages of baryon entrainment, first during the primary GRB stage, second during the interaction with the interstellar medium. The Fermi process works because of the Brillouin backscattering process that turns out to be appropriate and efficient, moreover it allows the heating and deceleration of the shell plasma by the incoming flux. Although the primary

stage does not produce UHE cosmic rays because of synchrotron losses, the Fermi acceleration allows the maintenance of a high energy proton population between R_h and R_{pp} that can emit a significant low energy neutrino flux of the order $10^{-2} E$. A high energy neutrino flux can be generated through the $p\gamma$ -process by UHE cosmic rays at the end of the free expansion, typically a sizable fraction of the UHE cosmic ray energy in the form of $10^{14}-10^{16} eV$ neutrinos (Rachen & Mészáros 1998).

Acknowledgements. The authors are grateful to Y. Gallant, G. Henri, A. Marcowith, R. Mochkovitch and J. Rachen for fruitful discussions.

References

- Aharonian F.A., Cronin J.W., 1994, Phys. Rev. D 50, 1892
 Blandford R.D., McKee C.F., 1976, Phys. Fluids 19, 1130
 Champeaux S., Laveder D., Passot T., Sulem P.L., 1999, Nonlinear Processes in Geophysics 6, 169
 Daigne F., Mochkovitch R., 1998, MNRAS 296, 275
 Gallant Y., Achterberg A., 1999, MNRAS 305, L6
 Hayashida N., Honda K., Inoue N., et al., 1998, In: Paul J., Montmerle T., Aubourg E. (eds.) Abstracts of the 19th Texas Symposium on Relativistic Astrophysics and Cosmology, held in Paris, France, Dec. 14–18, 1998, CEA Saclay
 Marcowith A., Pelletier G., Henri G., 1997, A&A 323, 271
 Paczynski B., Xu G., 1994, ApJ 427, 708
 Pelletier G., 1999, A&A 350, 705
 Pelletier G., Marcowith A., 1998, ApJ 502, 598
 Rachen J., Mészáros P., 1998, Phys. Rev. D 58, 123005
 Rees M.J., Mészáros P., 1992, MNRAS 258, 41
 Sokolsky P., 1998, In: Paul J., Montmerle T., Aubourg E. (eds.) Abstracts of the 19th Texas Symposium on Relativistic Astrophysics and Cosmology, held in Paris, France, Dec. 14–18, 1998, CEA Saclay
 Vietri M., 1995, ApJ 453, 883
 Waxman E., 1995, ApJ 452, L1
 Waxman E., Bahcall J.N., 1999, Phys. Rev. D 59, 023002